RSS-based Carrier Sensing and Interference Estimation in 802.11 Wireless Networks

Jeongkeun Lee*, Sung-Ju Lee†, Wonho Kim*, Daehyung Jo*, Taekyoung Kwon*, and Yanghee Choi*

*School of Computer Science and Engineering, Seoul National University, Korea
†Mobile and Media Systems Lab, Hewlett-Packard Laboratories, Palo Alto, USA
Email: {jklee,whkim,cdh}@mmlab.snu.ac.kr, sjlee@hp.com, {tkkwon,yhchoi}@snu.ac.kr

***Abstract*—We analyze the carrier sensing and interference relations between the two wireless links and measure the impact of these relations on link capacity in two indoor 802.11a mesh network testbeds. We show that asymmetric carrier sensing and/or interference relations happen frequently in wireless networks; these asymmetric relations affect not only the level of performance degradation, but also the fairness of channel access. We then propose a new methodology that predicts the relation of carrier sensing and interference based on radio signal strength measurements. The measurement complexity increases only linearly with the number of wireless nodes. To our knowledge, the proposed methodology is the first trial that considers physical layer capture, and detects the source of interference that is out of the communication range. We validate the prediction methodology on an 11-node wireless mesh network testbed.**

***Index Terms*—Carrier Sensing, Interference, Asymmetric Links, Wireless Networks**

I. Introduction

Estimating carrier sensing and interference in wireless networks is a challenging task. Most papers have predicted the interference and carrier sensing (CS) ranges based on the distance between the nodes. However, measurement results [1] show that the distance does not have a strong correlation with the quality of the wireless links (e.g., received signal strength (RSS)). Moreover, most of the existing work presumes the CS range is always symmetric between the two nodes. However in some cases, one sender senses the other sender's transmission but not vice versa. One of the key contribution of this paper is that we observe and quantify the substantial existence of the *asymmetric* CS relation.

We first study interference on 802.11 wireless networks by investigating its relation with carrier sensing. We categorize their relations on two wireless links and carry out testbed experiments to evaluate their effect on the link throughput and goodput.[2] From our indoor 802.11a testbed measurements, we show that asymmetric CS and asymmetric interference relations happen frequently in a real wireless network. We enumerate a total of 16 topology cases of four CS relations and four interference relations between the two links. Based on the distinctive performance characteristics, we classify these 16 cases into five groups, among which three groups show severe unfairness or aggregate goodput degradation. From our experiments on two separate testbeds, 46% and 72% of the link pairs in the two networks fall into these three groups, respectively.

We then propose a RSS-based prediction (RBP) methodology that estimates the CS and interference relations between any given two links in the network. Based on our thorough experimental investigation on carrier sensing and physical layer capture (PLC), we suggest a measurement-based CS and interference model as a function of an RSS. In particular, we observe that PLC and interference threshold is affected by the CS relation and this finding is considered into the interference prediction component of RBP. RBP requires hello broadcast from each node with two different power levels only at the network instantiation. Thus, our scheme generates $2n$ message overhead, where n is the number of the

This work was supported in part by the Hewlett-Packard Laboratories University Relations Program, the National Information Society Agency (NIA) of Korea, and the Brain Korea 21 project of the Ministry of Education, Korea.

[2]We distinguish between the throughput at a transmitter (TX) and the goodput at a receiver (RX). Throughput is defined as the rate of bytes transmitted at the sender's application whereas goodput is defined as the rate of bytes received at the receiver's application. In the presence of interference, RX goodput is less than TX throughput.

1-4244-1268-4/07/$25.00 ©2007 IEEE

This full text paper was peer reviewed at the direction of IEEE Communications Society subject matter experts for publication in the IEEE SECON 2007 proceedings.

nodes in a wireless network. This linear measurement complexity is one of the advantages of the proposed scheme. Moreover, the use of two power levels for hellos locates the source of hidden interference even when the interferer resides outside of the communication range.

Our contributions are the following: (i) we measure the effect of CS and interference on both unicast and broadcast traffic, (ii) we estimate the degree of CS and interference and the goodput of each link pair, (iii) we demonstrate the substantial existence of the asymmetric CS relation and its effect on interference, (iv) we consider the physical layer capture in interference prediction, and (v) we detect out-of-range hidden interferers.

II. Related Work

Estimating interference is important yet difficult in wireless networks. There has been numerous work on this topic. Here we focus on those that are the most relevant. Link Interference Ratio (LIR) and Broadcast Interference Ratio (BIR) [2] are one of the first *measurement-based*, instead of distance-based, schemes that estimate interference between two wireless links that do not share end-points. Both LIR and BIR, with different measurement complexities, accurately estimate the amount of pairwise link interference. However, as will be shown in Section IV, they do not indicate the fairness between the two links. They cannot differentiate cases when a link dominates the medium from when both links share the channel equally, as long as the aggregate goodput of the two links of both cases are the same.

The two link topology classification based on link geometry is introduced in [3]. It modeled the unicast performance and short-term fluctuation between the two links and expanded the model to consider per-link performance behavior in [4]. Although their topology analysis and performance modeling provide a deep understanding of the behavior of CSMA protocols in various network topologies, their experiment is limited to simulation and do not consider asymmetric carrier sensing. Estimation of interference is not dealt in their work.

A recent work [5] tries to achieve a similar goal of estimating the interference and broadcast goodput based on RSS measurements. The difference is that we analyze interference/carrier-sensing relationship with unicast/broadcast measurements and use the measurement-based categorization to predict unicast goodput. Moreover, we introduce novel findings from asymmetric carrier sensing between the nodes and we use them to enhance the interference prediction. We also consider the interference caused by the nodes outside the communication range, which cannot be predicted by normal-power hello exchanges.

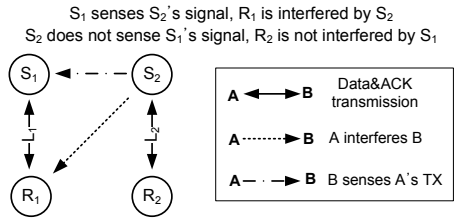

Fig. 1. Example of carrier sensing and interference between link L_1 and link L_2.

Our previous work [6] introduced how to quantify levels of carrier sensing and interference. We proposed methods to estimate broadcast throughput and goodput based on the quantifying metrics. This work provided a basis for our prediction methodology in Section V.

III. Carrier Sense and Interference Relation

A. Definitions

In order to define CS and interference relations, we consider two directed links L_1 and L_2 that do not share end-points. On L_1 and L_2, nodes S_1 and S_2 transmit data to nodes R_1 and R_2 respectively, as illustrated in Fig. 1. Arrows in the figure indicate the directions of data/ACK packets, interference signals, and sensed signals. The CS relation between the two links is decided by S_1 and S_2, while the interference relation depends on how the sender of one link affects the communication of the other link: S_1's effect on L_2, and S_2's effect on L_1.

1) CS Relation: In the CS mechanism, a wireless station withholds its transmission when it senses an ongoing transmission on the medium. In Fig. 1, when S_1 senses S_2's transmission, a CS relation exists between the two links and we say L_2 is carrier sensed by L_1. Note that in 802.11a systems, the energy-detection carrier sensing threshold is set to be 20 dB above the minimum 6 Mbps reception sensitivity: a CS range is equal to or smaller than the packet communication range, while the CS range in 802.11b systems is larger than the communication range according to the standard [7].

As shown in Fig. 1, there can exist an *asymmetric* CS relation between the two nodes. In our testbed network deployed in HP Labs in Palo Alto, CA, 17% of the node pairs exhibits asymmetric CS relation. Among the node pairs, 14% had mutual CS relation while 69% do not sense each other in any direction.

2) Interference Relation: We define the interference relation independently of the CS relation. In Fig. 1, if

S_2's simultaneous transmission with S_1 hinders R_1's successful reception of S_1's packet, we say L_1 is interfered by L_2 (or S_2). In reality, if both S_1 and S_2 sense each other, they do not transmit simultaneously assuming the adequate carrier sensing and collision avoidance mechanisms. We however define the interference relation independently of the CS relation for the simplicity of case enumeration.

Interference becomes effective when the signal-to-interference/noise-ratio (SINR) at R_1 goes below the required value due to S_2's transmission. By ignoring the noise power which is usually much weaker than the intended signal (typically up to 70dB difference), the SINR becomes the signal-to-interference-ratio (SIR). The SIR at R_1 is defined as "RSS from S_1 *minus* RSS from S_2" where RSS is given in dBm and SIR is in dB scale. If the SIR is below a threshold, S_2 effectively interferes R_1's reception of packets from S_1. In Section V, we show that the SIR threshold is highly affected by the CS relation.

Note that R_1's being able to receive a S_2's packet does not necessarily mean R_1 is interfered by S_2. Its converse is not true, either. For example, if S_1 is much closer to R_1 than S_2 is, R_1 can still decode the packets from S_1 despite the interferer S2. In general, interference is determined by the SIR relation between the two senders and one receiver. Thus, estimating interference (and also CS) solely based on the existence of a communication link, which is popular in the literature, is not accurate.

As we consider a large data payload (about 1000 bytes), we ignore the interference caused by ACK packets (14 bytes). Supporting observations have been made in [2]. This simplification helps us focus on the interaction between CS and inter-data packet interference. It is elaborated in [3], [4] that ACK-DATA collisions cause considerable performance degradation only when each receiver is not interfered by the sender of the other link, i.e., when there is no interference between data packets.

3) State Representation of CS and Interference: Although carrier sensing and interference are not binary [6] (also to be shown in Section V) and should be represented in continuous values, we consider a binary (yes or no) state for both CS and interference for simplicity. If S_1 can sense S_2's transmission, the carrier sensing state of L_1 by L_2 is expressed as $C_1{:}Y$, and otherwise $C_1{:}N$. Similarly, if L_1 suffers interference from L_2 (or S_2), the interference state of L_1 by L_2 is $F_1{:}Y$, and otherwise $F_1{:}N$. In the example in Fig. 1, L_1's state by L_2 is $C_1{:}Y$ / $F_1{:}Y$ and the state of L_2 by L_1 is $C_2{:}N$ / $F_2{:}N$.

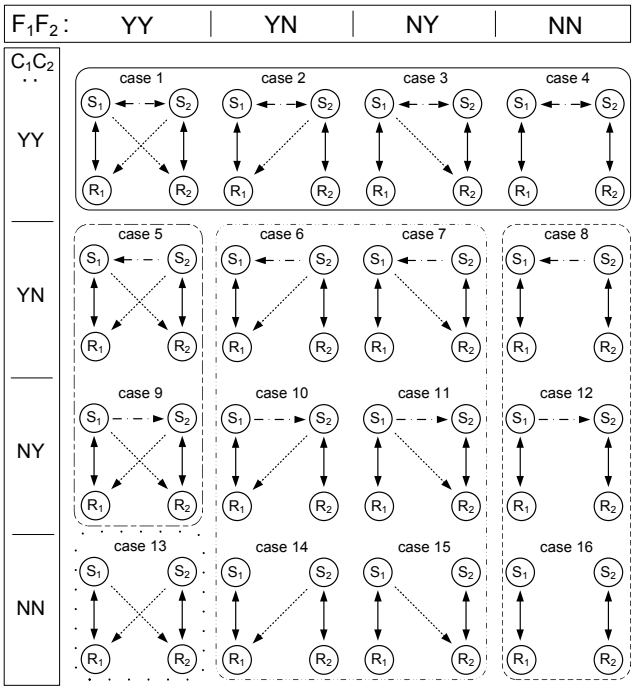

Fig. 2. 16 topology cases between the two links.

B. Two Link Topologies and Classification

Because each of the CS and interference relations between the two links has four states YY, YN, NY, NN, there are $4 \times 4 = 16$ topology cases, as depicted in Fig. 2. Based on their distinctive performance characteristics, we classify them into five groups as follows.

1. Mutual CS : cases 1-3, where both senders sense each other. Note that case 4 also falls in this group, but we put this case into group 2 for the simplicity of presentation.
2. No interference (INT) : cases 4, 8, 12, and 16, where both links are free from interference.
3. One-way hidden INT : cases 6, 7, 10, 11, 14, and 15, where one of the two links suffers from interference.[3]
4. Mutual INT, asymmetric CS : cases 5 and 9, where respective link is interfered by the other link, but only one sender senses the other sender.
5. Mutually hidden INT : case 13, in which both senders are hidden from the other and both links interfere each other.

IV. Measurement Study of Carrier Sensing and Interference on Two Saturated Links

We embodied 16 network topologies corresponding to Fig. 2 on our testbed. The operational wireless com-

[3]We explain later why cases 6 and 11 are included in this group.

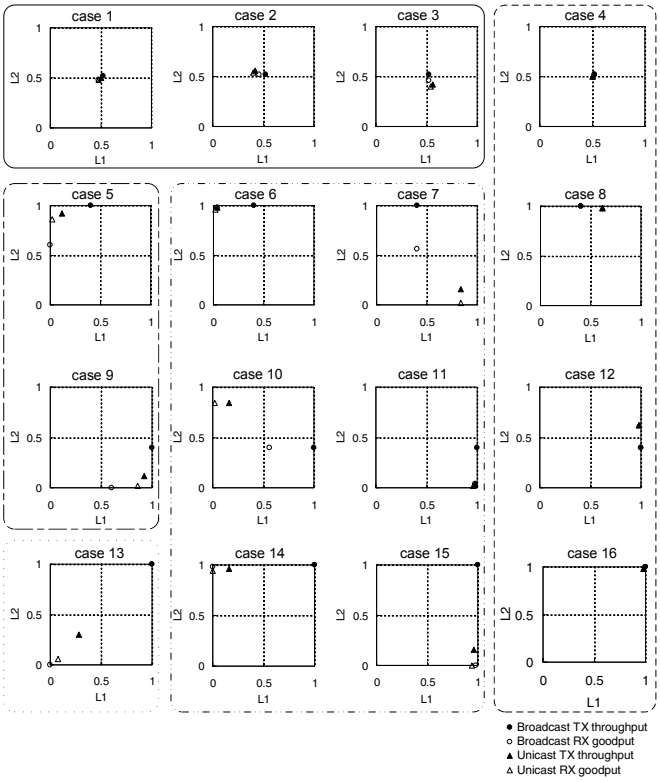

Fig. 3. Normalized link throughput/goodput of two saturated links.

munity network solution [8] is installed to allow mesh connectivity and routing for small-form factor single-board computers [9] with mini-PCI 802.11a cards using Atheros chipset [10]. To embody each topology case with different CS and interference relation, we controlled the node placement, transmission power, and transmission/reception antennas. The applications on S_1 and S_2 generate UDP packets of 1000 bytes and continuously send them to R_1 and R_2 respectively, to make their output queue always backlogged (saturated). During the entire experiments, the PHY rate is fixed at 6 Mbps, which is the lowest and the most robust bit rate in IEEE 802.11a. We used a clear 802.11a channel to avoid interference from other networks.[4] Each broadcast/unicast transmission period was 30 seconds.

We first measure *interference-free* TX throughput (sending traffic rate at a sender's application) and RX goodput (traffic rate successfully delivered to a receiver's application) by activating a link while deactivating all other links in the network.[5] Because of the PHY/MAC overhead, the measured interference-free throughput/goodput is 5.1 Mbps for broadcast and 4.9 Mbps for unicast. We call those values as the *channel capacity* for broadcast and unicast (of 6 Mbps PHY rate) throughout this paper.

For each 16 topology cases, we measured the throughput and the goodput of UDP broadcast and unicast of L_1 and L_2 when both links are simultaneously active and the input traffic is always backlogged. We verified that each link's interference-free throughput and goodput reach the channel capacity before testing the simultaneous transmissions. We normalized the measured throughput and goodput by the channel capacity and plot them in Fig. 3. We now analyze the unique performance characteristics of the five groups classified in Fig. 2.

A. Mutual Carrier Sensing (cases 1, 2, 3)

In this group, both senders sense each other. Thus, both links have a fair share of broadcast/unicast throughput/goodput as shown in Fig. 3. As we consider the fixed payload size and PHY rate, ideally, each sender of two mutually sensing senders must have equal transmission opportunity and equal share of TX throughput, which is a half of the channel capacity. Because both senders are not perfectly slot-synchronized and they can choose the same random counter number, they might however transmit simultaneously. That is why their broadcast TX throughput are little larger than 0.5. A collision may occur between the simultaneous transmissions if the interference state is Y: in case 2 for instance, L_1's broadcast goodput is smaller than broadcast throughput while L_2's goodput is equal to throughput.

For unicast packets, retransmission and exponential backoff mechanism is applied: if no ACK is received for the transmitted data packet, the sender doubles the CW and counts down before retransmitting the packet, where CW is the contention window size in slot numbers. Thus, if a collision occurs, not only RX goodput but also TX throughput decreases because of the increased countdown (backoff) time. For the example of case 2, L_1's unicast throughput and goodput are smaller than 0.5 while L_2's are larger than 0.5. Because L_2's interference state is N, it does not suffer from collision and backoff, and it gets more chance to transmit when L_1 increases its CW and yields the channel.

B. No Interference (cases 4, 8, 12, 16)

Because both links in this group are free from interference, goodput is the same with throughput for every cases. Analyzing this group helps us understand the

[4]The wireless network deployed by the IT runs 802.11b/g.

[5]In order to have accurate throughput/goodput measurement at the application layer, we eliminated the effect of UDP buffer queueing time on the throughput measurement and maximized the application process priority.

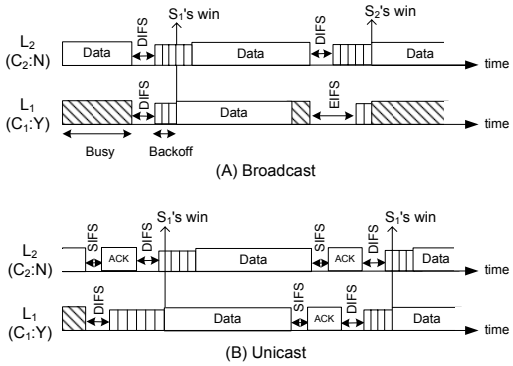

Fig. 4. Timing examples of asymmetric CS.

effects of (especially asymmetric) carrier sensing on TX throughput.

Cases 4 and 16 show the expected results: when both senders sense each other, two links equally share the channel capacity; and when two links operate independently, both links fully use the channel capacity.

When CS relation is asymmetric, the normalized throughput of the sender that does not sense the other sender is one as expected. The throughput of the carrier sensing sender however, differs from expectation which is about 0.5.

For broadcast, TX throughput is 0.4 (smaller than 0.5) while it is 0.63 for unicast as shown in cases 8 and 12. For broadcast, we identify Extended Inter-Frame Spacing (EIFS) of 802.11 as the cause. In 802.11 MAC, a node that has received a packet that it could not decode must go into the EIFS mode and waits until either receiving an error-free frame or the expiration of the EIFS time which is larger than the double of DIFS time in 802.11a. Using case 8 as an example, the carrier sensing sender S_1 transmits a broadcast data when it chooses a backoff counter that is smaller than S_2's as illustrated in Fig. 4 (A). Because S_2 does not sense S_1's transmission, it also starts its transmission. As S_2's transmission starts later then S_1's, S_1 senses the latter part of S_2's transmission after finishing its own transmission and goes into the EIFS mode. Because S_1 missed the preamble and the PHY header of S_2's packet, S_1 is unable to decode the S_2's packet. While S_1 waits for EIFS duration, S_2 begins its backoff counter earlier than S_1, which increases the possibility that S_2 begins the next transmission ahead of S_1's backoff counter expiration. In this manner, S_1, the sender that carrier senses, has transmission probability less than 0.5 after its previous transmission.

When unicast traffic is examined, we have a different scenario as illustrated in Fig. 4 (B). In the above example of the transmission of carrier sensing sender S_1, it receives an ACK from its receiver R_1 after its data transmission. It is highly unlikely that S_1 senses the latter part of S_2's transmission and goes into the EIFS mode. Furthermore, as S_1 does not sense R_2's ACK transmission, it decrements its backoff counter while S_2 is receiving an ACK from R_2. Hence for unicast transmission, S_1 has a transmission probability larger than 0.5 not only after its previous transmission (second "S_1's win" in Fig. 4 (B)) but also after yielding the channel by sensing S_2's data transmission (first "S_1's win"). We confirmed the above arguments by observing the transmission order and inter-transmission time of S_1 and S_2 by using an 802.11 packet sniffer.

C. One-way Hidden Interference (cases 6, 7, 10, 11, 14, 15)

In this group where link pairs have asymmetric interference relations and at least one $C : N$ state, severe goodput unfairness between the two links is exhibited. In particular, the link whose interference state is $F : Y$ has almost zero unicast goodput while the other link's unicast goodput is close to one. From this result, we can take two lessons.

1) Hidden node problem occurs no matter which sender is hidden: We observe that a link is interfered when at least one of the senders of the link pair is hidden; either the sender of the link or the interfering sender of the other link (i.e., C_1C_2 is YN, NY, or NN). Thus, the commonly used term *hidden interference* should differentiate two cases: (1) the sender is hidden from the interferer (e.g., in case 6, the sender S_1 is hidden from its interferer S_2 and L_1 has almost zero unicast goodput), and (2) the interferer is hidden from the sender (e.g., in case 10, the interferer S_2 is hidden and L_1 has almost zero unicast goodput).

2) The winner takes it all: The interference-free (F:N) link takes most, if not all, of the channel capacity with unicast traffic. This is evident in cases 7 and 10, where the broadcast goodput result shows a nearly fair share between the two links whereas the unicast goodput share is extremely unfair. It is due to the exponential backoff mechanism, which form a vicious cycle in case 10 for example as follows:

1. The sender S_1 of the interfered link L_1 increases its CW when it does not receive an ACK from R_1.
2. S_1's packet transmission rate decreases.
3. S_2 gets more chances to transmit while S_1 refrains its transmission due to the increased CW. S_2's TX throughput hence increases.

4. As the interferer S_2's TX throughput increases, the packet drop rate of L_1 increases, and S_1's CW is again doubled.

As the above cycle repeats, L_1's unicast RX goodput drastically drops and reaches near zero while L_2 takes most of the channel capacity. Note that this result contrasts that of broadcast. Because there is no explicit ACK mechanism for broadcast packets, the sender does not know whether its broadcast packet is collided and does not perform backoff. That is why the broadcast TX throughput of the interfered links does not decrease despite packet collisions resulting from interference.

D. Mutual Interference & Asymmetric Carrier Sensing (cases 5, 9)

When both links interfere with each other and the CS relation is asymmetric, the link that does *not* sense takes most of the channel capacity. The link sensing the other link's transmission, for example L_1 in case 5, begins to yield the channel which in turn decreases the other link L_2's collision probability. L_1's collision probability however, remains high as L_2 does not sense L_1 and does not yield the channel. S_1's CW thus increases faster than S_2's. L_2 takes most of the channel capacity and L_1's goodput reaches almost zero.

E. Mutual Hidden Interference (case 13)

We observe poor performance from both links when they interfere with each other and the sources are hidden from each other. The goodput degradation becomes intensified because of the saturated traffic from both senders. This topology scenario occurs quite frequently as 22% of the link pairs in our Palo Alto testbed fall into this category. By applying the model of [11] to our 802.11 testbed, we found that our measurement results follow the model and the performance degradation gets intensified when a larger payload size is used.

F. Occurrence Frequency

We measured how frequently each group occurs in our 10-node testbed in HP labs (HPL). We also have an 11-node testbed deployed over a floor of a building in Seoul National University (SNU).

We choose a pair of links where each link has greater than 0.5 normalized interference-free unicast goodput. We found a total of 152 and 116 such pairs in HPL testbed and in SNU testbed, respectively. Since HPL building is an open space with cubicles, the HPL testbed has more links between nodes than the SNU testbed which is deployed over office rooms with thick concrete walls. Table I shows the percentage of each group occurring in our testbed. Note that we examine link pairs and not node pairs.

TABLE I
OCCURRENCE FREQUENCY OF EACH GROUP.

	HPL	SNU
Mutual CS	39%	9%
No INT	15%	19%
One-way hidden INT	21%	55%
Mutual INT & Asymmetric CS	3%	2%
Mutual hidden INT	22%	15%

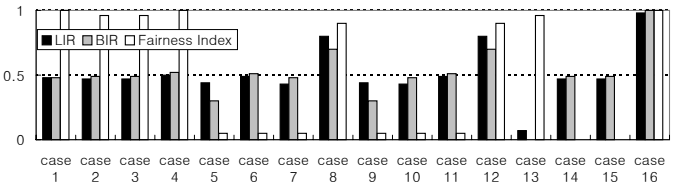

Fig. 5. LIR, BIR and goodput fairness index of 16 cases.

G. LIR and BIR Analysis

LIR [2] between the two links L_1 and L_2 is defined as $LIR = \frac{P_1'+P_2'}{P_1+P_2}$ where P_1 and P_2 denote the link goodput of L_1 and L_2 when each link is active individually, and P_1' and P_2' are goodputs when both links are are active simultaneously. LIR takes a value between 0 and 1. $LIR = 1$ indicates no interference between the two links. A network with n nodes has $O(n^2)$ links, and as pairwise interference is measured to calculate LIR, message overhead is $O(n^4)$.

Broadcast Interference Ratio (BIR) [2] is proposed to reduce the trial overhead. BIR is defined similar to LIR except a pair of senders broadcast instead of unicast. All neighbor nodes measure the goodput from each two broadcasting nodes, which result in $O(n^2)$ combinations with every pair of senders examined. It is shown that BIR predicts pairwise link interference as accurate as LIR [2]. Our measurement data also support this argument in Fig. 5. However, BIR and LIR do not indicate the goodput of each link and fairness between the links. For example, BIR=0.5 or LIR=0.5 cannot differentiate between (i) when one link has the entire goodput and the other link receives none, and (ii) when both links share equal goodput. To show this, we use Jain's fairness index $ind = \frac{(P_1'+P_2')^2}{2(P_1'^2+P_2'^2)}$. With this definition, the minimum index value is 0.5 when the goodput share is extremely unfair between the two links. We modify it as $(ind-0.5)\times 2$ and use it in Fig. 5. The modified index ranges from zero (extreme unfairness) to one (perfect fair share between the two links). We

can observe the low fairness index for the links with the asymmetric CS relation (cases 5, 6, 7, 9, 10, and 11).

V. RSS Based Prediction (RBP)

We have shown that the goodput behavior of a pair of links can be explained by the CS and interference relation. We now propose a method to predict the CS and interference relation between the two given links. In addition, it estimates the goodput of each link and hence the fairness between the links. Our scheme requires only $O(n)$ message overhead.

Our methodology is based on RSS measurement, and hence named RSS based prediction (RBP). We use a centralized coordinator that collects measurement data from each mesh node and performs the estimation.[6]

A. RSS Measurement Methodology

1) High-power/Normal-power channel probing: Every mesh node broadcasts hello messages at the lowest PHY rate (6 Mbps in our 802.11a testbed) at a scheduled time and measures RSSs from the neighboring nodes. With commodity 802.11 wireless LAN cards, we obtain an RSS value when the received packet is correctly decoded. Thus, those nodes that are within an estimating node's interference range but outside its reception range cannot be accounted for in the RSS measurements. To address this problem, we use high-power (HP) and normal-power (NP) hello broadcast as introduced in Radio Interference Detection (RID) [12]. Each node performs hello broadcast twice; once each with high and normal power levels. The NP level is used for actual data communications, and HP is Y dB higher than the NP level. If a NP hello is received, its RSS is measured and reported to the coordinator. If only a HP hello is received, the node measures its RSS, subtracts Y dB, and reports the result to the coordinator.

Our testbed measurements show that the RSS difference between the HP and the NP packets follows a normal distribution $\mathcal{N}(10, 1.3)$.

Once the RSSs are collected, the coordinator predicts the CS and interference relation for each link pairs, as described in the following subsections. Although we have assumed the CS and interference states as binary to explain the 16 cases, both CS and interference have certain transition ranges in terms of RSS and SIR respectively, and they exhibit intermittent state in those ranges. Thus from now on, we use the terms c_i and f_i as CS and interference metrics having continuous values $[0, 1]$ instead of binary CS and interference states C_i and F_i.

[6]Clearly, a centralized solution has limited scalability. However, in an indoor mesh network such as a home or an enterprise network, the network size is relatively small. Moreover, having a coordinator makes the implementation simple and enables accurate prediction. In our testbed configuration, the coordinator server is located outside of the mesh network although any mesh node can perform as the coordinator.

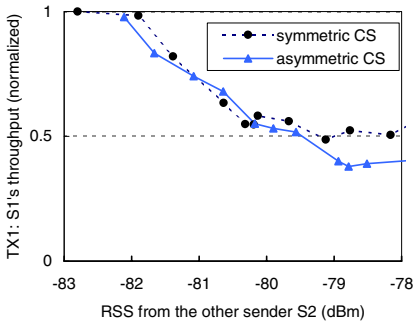

Fig. 6. Carrier Sensing vs. RSS.

B. Carrier Sensing and TX Throughput Prediction

Fig. 6 plots the broadcast TX throughput TX_1 of sender S_1 (normalized over the broadcast channel capacity) versus the RSS of packets received from the other sender S_2, which is varying its transmission power.[7] Fig. 6 shows the two cases: symmetric CS when S_2 is always sensing S_1 completely (c_2 is one), and asymmetric CS when S_2 is not sensing S_1 at all (c_2 is zero). As S_2 varies its transmission power, c_1 is varied from zero to one. Our goal is to get the estimation of c_1, $\hat{c_1}$, based on RSS of S_2's hellos received at S_1 and to estimate TX_1 using $\hat{c_1}$ and $\hat{c_2}$.[8]

In the symmetric CS case, TX_1 begins to decrease when RSS from S_2 is -82 dBm and stops decreasing and converges to 0.52 when RSS is -79 dBm. TX_1 of the asymmetric CS case shows similar monotonic decrease but becomes 0.4 when S_1 carrier senses S_2 completely at -79 dBm. Remember that the analysis of the converging throughput points were given at Sections IV-A (the backoff countdown race) and IV-B (the EIFS effect). We obtained very similar shape of plots for other node pair experiments and hence use -82 dBm and -79 dBm as CS thresholds RSS_{low} and RSS_{high}.

In the RBP methodology, when a node pair S_1 and S_2 is given, the CS metric $\hat{c_1}$ of S_1 is estimated by using the RSS of hellos received from S_2 at S_1, which we denote as r_1. We consider the function linearly increasing

[7]We enabled a per-packet power control at the application socket layer by modifying the Atheros driver and the netBSD kernel.

[8]Here we assume that $\hat{c_2}$ is given. However, we can calculate $\hat{c_1}$ and $\hat{c_2}$ simultaneously by solving simple simultaneous equations as shown in Section VI.

from 0 to 1 in the transition range $[RSS_{\text{low}}, RSS_{\text{high}}]$ as follows:

$$\hat{c_1} = \begin{cases} 0 & \text{if } r_1 \leq RSS_{\text{low}} \\ \frac{r_1 - RSS_{\text{low}}}{RSS_{\text{high}} - RSS_{\text{low}}} & \text{if } RSS_{\text{low}} < r_1 \leq RSS_{\text{high}} \\ 1 & \text{if } r_1 > RSS_{\text{high}}. \end{cases}$$

Because we can consider $\hat{c_1}$ as the probability of S_1 yielding the channel, we can estimate the broadcast TX throughput of S_1, $\widehat{TX_1}$. We define $TX_{\text{def},1}$ as the amount of (normalized) throughput that S_1 defers when it completely senses S_2, i.e. when c_1 is one. Then, $\widehat{TX_1}$ is given as $\widehat{TX_1} = 1 - \hat{c_1} \cdot TX_{\text{def},1}$.

From Fig. 6, we have two different values of $TX_{\text{def},1}$ (1-0.52=0.48 and 1-0.4=0.6), depending on S_2's CS state. Thus, we define $TX_{\text{def},1}$ as a linear function of $\hat{c_2}$ as $TX_{\text{def},1} = 0.6 - (0.6 - 0.48) \cdot \hat{c_2}$.

C. Interference and RX Goodput Prediction

We derive the interference metric $\hat{f}$ using the interference versus SIR relation shown in Fig. 7. Given a link L_1:$S_1 \rightarrow R_1$ and an interfering sender S_2, we calculate SIR at R_1 as $sir_1 = r_{11} - r_{21}$ in dB scale where r_{ij} denotes RSS at R_j from S_i.[9] To generate various SIR values at the receiver, we controlled either or both of the two senders' transmission power as needed. We experimented with different methodologies in creating varying SIR values: changing the transmission power of the sender while keeping it constant for the interferer, and holding the transmission power of the sender constant while varying the power of the interferer. Our measurement showed that different methods have little impact on the relation between interference and SIR.

Fig. 7 shows that we have different transition ranges as the carrier sensing relation between the senders changes. When both senders are sensing each other, the effect of interference becomes negligible as shown in the *mutual CS* group of Section IV.

The difference between the plots in Fig. 7 results from the physical layer capture (PLC) in 802.11. PLC occurs when the stronger packet arrives before the weaker packet or the stronger packet arrives later but within the physical layer preamble of the weaker packet [13]. This PLC case happens in Fig. 7 (A) where only S_1 senses the other ($c_1 = 1$). R_1's RX goodput RX_1 ranges from nearly zero to 0.4 with a SIR transition range $[-2, 3]$. RX_1 can not exceed 0.4 because TX_1 is 0.4 in this asymmetric CS relation. Because S_1 transmits only when it wins or ties in the contention against S_2, S_1's packet satisfies the PLC condition when $SIR > 0$ as it arrives at the receiver before S_2's packet. W e can see the relatively rapid increase of RX_1 at $SIR = 0$.

Fig. 7 (B) shows that when only the interferer S_2 senses S_1, RX_1 ranges from 0.6 to one with a SIR transition range $[9, 11]$. Because TX_2 of the interferer S_2 can not exceed 0.4 in this asymmetric CS relation, RX_1 does not decrease below 0.6 even when it is interfered. The carrier sensing sender S_2 most of the time transmits before S_1 as it transmits only when it wins or ties in the countdown race against S_1. Thus S_1's packets mostly arrive at R_1 later than S_2's transmission (but within the maximum backoff time). In some 802.11 chips including Atheros, when a new packet with sufficiently stronger power arrives (say, 10 dB margin) in the midst of receiving the first packet, the receiver switches to receive the new packet [14]. This so-called "restart mode" operation explains the narrow transition range centered at 10 dB SIR.

When there is no CS between the senders, RX_1 ranges from zero to one with a wide SIR transition range $[12, 24]$, as shown in Fig. 7 (C). In the previous case where only S_2 senses, R_1 can listen the beginning of S_2's packet without being interfered by S_1 and synchronizes its receiver to S_2's signal although it may later switch to S_1's signal. Because transmissions of the two senders are completely asynchronous in this case of Fig. 7 (C), most of S_2's packet transmissions begin in the midst of S_1's transmission (and vice versa). R_1 is not able to decode the physical layer preamble and the PLCP header of S_2's packets and does not synchronize and lock onto S_2's packets. Therefore, when the stronger packets from S_1 arrives at R_1, R_1 is not decoding the S_2's packet and S_2's signal acts as noise at the R_1's receiver. This noise requires the receiver to have higher SIR to lock onto or capture S_1's signal. As mutual hidden interference occurs frequently (see Table I), utilizing the capture effect is important for wireless network capacity improvement.

To predict interference and derive the metric f_1, we consider the function linearly decreasing from 1 to 0 in the transition range $[SIR_{\text{low}}, SIR_{\text{high}}]$:

$$\hat{f_1} = \begin{cases} 1 & \text{if } sir_1 \leq SIR_{\text{low}} \\ \frac{sir_1 - SIR_{\text{low}}}{SIR_{\text{high}} - SIR_{\text{low}}} & \text{if } SIR_{\text{low}} < sir_1 \leq SIR_{\text{high}} \\ 0 & \text{if } r_1 > SIR_{\text{high}}. \end{cases}$$

To choose the appropriate values for SIR_{low} and SIR_{high}, we compare the CS metrics c_1 and c_2 to 0.5 and determine the binary CS state. For example, if $c_1 < 0.5$ and $c_2 \geq 0.5$, this is the case when only the interferer S_2

[9]Note the term r_i was used in the previous subsection to denote RSS at S_i from the other sender S_j.

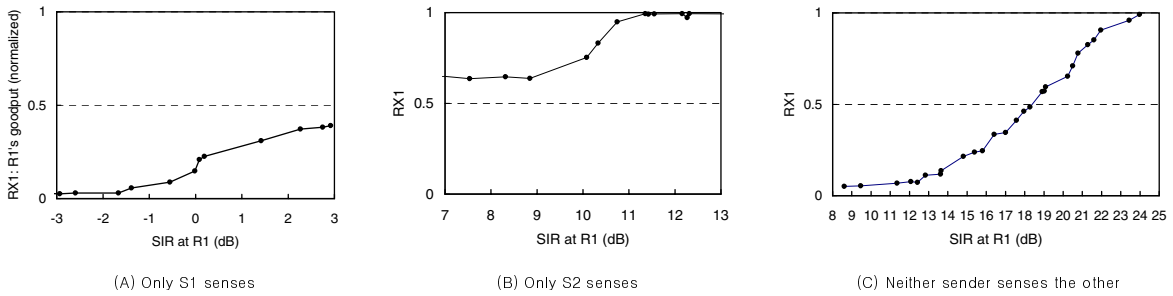

Fig. 7. Interference vs. SIR with various CS relation.

carrier senses: we use $SIR_{\text{low}} = 9$ and $SIR_{\text{high}} = 11$ from Fig. 7 (b). When both c_1 and c_2 are 0.5 or greater, we do not predict f_1.

Once we have $\hat{c_1}$, $\hat{c_2}$, and $\hat{f_1}$, we can estimate the broadcast RX goodput of link L_1 with interferer S_2. We take $\widehat{TX_1} + \widehat{TX_2} - 1$ as the fraction of the packets transmitted by the both senders simultaneously. The fraction of the packets successfully received at R_1, i.e., the RX goodput $\widehat{RX_1}$ is estimated as $\widehat{RX_1} = \widehat{TX_1} - \hat{f_1} \cdot (\widehat{TX_1} + \widehat{TX_2} - 1)$.

VI. Evaluation

We evaluate the accuracy of RBP on the 11-node 802.11a mesh network testbed in SNU. We observed similar results from the HPL testbed. We first perform hello broadcast for every node to transmit 200 hello packets twice with high-power and normal-power levels, which takes less than 3 minutes. This is the measurement time overhead of RBP in our instantiation. We predict the CS and interference metrics and link goodput based on the RSS of the hello exchanges. To verify the accuracy of RBP, we perform measurements for the node-pair carrier sensing test and the link-pair interference test. We excluded links whose packet delivery ratio (normalized broadcast RX goodput) is less than 0.5 for interference test using broadcast traffic. With unicast traffic, we use links whose normalized unicast RX goodput is greater than 0.8. The entire experiment took about 9 hours.

A. Carrier Sensing Prediction Evaluation

Based on our TX throughput prediction model, we compute the measured CS metric c_1 and c_2 for a given node pair. From Section V-B, we have closed-form equations $c_1 = \frac{1-TX_1}{0.6-0.12c_2}$ and $c_2 = \frac{1-TX_2}{0.6-0.12c_1}$ where TX_1 and TX_2 are the measured TX throughputs. If c (c_1 or c_2) is greater than one, we set c to one.

The comparison of the estimation $\hat{c_1}$ and the measurement c_1 is shown in Fig. 8. For the 110 directional node pairs in our 11-node testbed, the mean prediction error

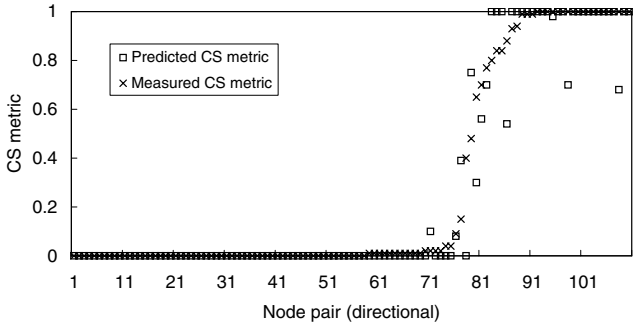

Fig. 8. Predicted and measured CS metrics of 110 node pairs.

is 0.03. Most prediction errors are concentrated in the carrier sensing transition range. We note that 13% of the node pairs exhibit asymmetric CS relation in SNU testbed and 17% in the HPL testbed.[10] These numbers support the significance of asymmetric CS study.

B. Interference Prediction Evaluation

We compute the measured INT metric f_1 and f_2 for a given link pair using our RX goodput prediction model. From Section V-C, $f_1 = \frac{TX_1 - RX_1}{TX_1 + TX_2 - 1}$ and $f_2 = \frac{TX_2 - RX_2}{TX_1 + TX_2 - 1}$ where RX_1 and RX_2 are the measured RX goodputs. If the computed f is larger than one, we set f as one. When both senders carrier sense, the effect of interference becomes negligible and we do not perform prediction.

Fig. 9 compares the estimations with the measured metrics. Our prediction shows high accuracy when there is no interference. However, we observe estimation errors when the interference is intermittent, especially when only normal-power hellos are used. Without the high-power (HP) hellos, RBP fails to detect interference on 30% of the link pairs (i.e., $\hat{f}$ is zero although $f > 0.5$). This results from the lack of RSS information of the interferer that is outside the receiver's communication range. When we use high-power hellos, interference of

[10]The continuous CS metric c is converted to a binary state: C:Y if $c > 0.5$ and C:N when $c \leq 0.5$. Asymmetric CS relation is formed when C_1 and C_2 are different.

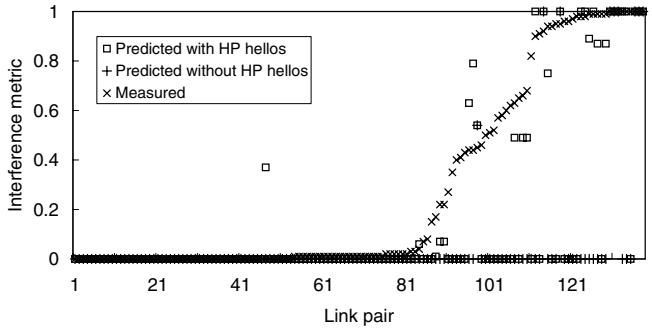

Fig. 9. Predicted and measured interference metrics for 138 link pairs. Most of "+" points are positioned at the bottom. Some "+" points after link pair number 121 are positioned at the top.

only 9% of the link pairs go undetected. With the high-power probing, the overall median and mean prediction error $|f - \hat{f}|$ is 0.01 and 0.14, respectively.

If we consider only the cases when prediction is possible, i.e., when RSSs from the both senders are available, the median error is zero and the mean error is 0.09 with high-power probing.

The prediction accuracy is relatively high when any of the two senders carrier senses while the accuracy decreases when neither sender senses the other. When both senders are hidden from each other, the interference versus SIR transition range is wider than other cases. We also observe more undetected interferers even with high-power probing.

C. Broadcast and Unicast Goodput

Based on the CS and interference predictions, we estimate the saturated goodput of each pair of links. Using the equations in Section V-C, our broadcast RX goodput prediction with high-power probing showed the median prediction error of 0.023 and the mean prediction error of 0.14.

For the saturated unicast goodput estimation, we use the observed goodput values of the 16 cases in Section IV. The predicted CS and interference metrics determine which one of the 16 cases matches to a given link pair and we use the goodput values in Fig. 3 as the estimation of the given link pair. The error between the estimations and the measurements exhibits zero median and 0.15 mean when we tested 75 pair of links whose interference-free goodput is greater than 0.8.

VII. Conclusion

We studied carrier sensing and interference relations using our testbed measurements, and investigated the impact of these relations on the capacity of the two 802.11a links. We presented Received Signal Strength (RSS) based prediction (RBP) that estimates the CS and interference relation between the two links and each link's goodput. Our scheme considers physical layer capture and locates the source of hidden interference even when the interferer resides outside of the communication range. We showed from our 11-node indoor testbed experiments that RBP effectively predicts the link behavior with $O(n)$ measurement overhead. Our future work includes testing RBP on networks with different wireless chipsets, investigating the capture effect on interference, and considering more than one interferer.

References

[1] K. Papagiannaki, M. Yarvis, and W. S. Conner, "Experimental Characterization of Home Wireless Networks and Design Implications," in *Proc. IEEE INFOCOM*, Barcelona, Spain, Apr. 2006.

[2] J. Padhye, S. Agarwal, V. Padmanabhan, L. Qiu, A. Rao, and B. Zill, "Estimation of Link Interference in Static Multi-hop Wireless Networks," in *Proc. ACM/USENIX Internet Measurement Conference (IMC)*, Berkeley, CA, USA, Oct. 2005.

[3] M. Garetto, J. Shi, and E. W. Knightly, "Modeling Media Access in Embedded Two-Flow Topologies of Multi-hop Wireless Networks," in *Proc. ACM MobiCom*, Cologne, Germany, Aug. 2005.

[4] M. Garetto, T. Salonidis, and E. W. Knightly, "Modeling Per-flow Throughput and Capturing Starvation in CSMA Multi-hop Wireless Networks," in *Proc. IEEE INFOCOM*, Barcelona, Spain, Apr. 2006.

[5] C. Reis, R. Mahajan, M. Rodrig, D. Wetherall, and J. Zahorjan, "Measurement-Based Models of Delivery and Interference. in Static Wireless Networks," in *Proc. ACM SIGCOMM*, Pisa, Italy, Sept. 2006.

[6] W. Kim, J. Lee, T. Kwon, S. Lee, and Y. Choi, "Quantifying the Interference Gray Zone in Wireless Networks: A Measurement Study," in *Proc. IEEE ICC 2007*, Glasgow, Scotland, June 2007.

[7] IEEE 802.11a, *Part 11: Wireless LAN Medium Access Control (MAC) and Physical Layer (PHY) specifications: High-speed Physical Layer in the 5 GHz Band*, Supplement to IEEE Std. 802.11, Sept. 1999.

[8] Champaign-Urbana community wireless network. http://www.cuwireless.net/.

[9] Soekris, inc. http://www.soekris.com/.

[10] Atheros Communications. http://www.atheros.com/.

[11] H. Chang and V. Misra, "802.11 Link Interference: A Simple Model and A Performance Enhancement," in *Proc. IFIP NETWORKING*, Waterloo, Canada, May 2005.

[12] G. Zhou, T. He, J. A. Stankovic, and T. F. Abdelzaher, "RID: Radio Interference Detection in Wireless Sensor Networks," in *Proc. IEEE INFOCOM*, Miami, FL, USA, Mar. 2005.

[13] A. Kochut, A. Vasan, A. Shankar, and A. Agrawala, "Sniffing out the correct physical layer capture model in 802.11b," in *Proc. IEEE ICNP*, Berlin, Germany, Oct. 2004.

[14] P. C. Ng and S. C. Liew, "Throughput Analysis of IEEE 802.11 Multi-hop Ad hoc Networks," *IEEE/ACM Trans. Networking*, June 2007.